# CROSS-SECTION OF γ-RAY PRODUCTION BY FAST NEUTRONS ON CADMIUM

**B.M. Bondar, V. M. Bondar, O. M. Gorbachenko, I. M. Kadenko, B. Yu. Leshchenko, Yu. M. Onishchuk, V. A. Plujko**

*Nuclear Physics Department, Taras Shevchenko National University, Kiev, Ukraine*

## Abstract

Measurements of prompt γ-ray yield produced by the interaction of 14 MeV neutrons with cadmium have been performed. Time-of-flight method based on pulse neutron generator was applied. Differential cross sections of $^{nat}Cd$ *(n, xγ)* reactions were unfolded from amplitude spectra and cross section uncertainties were estimated. Experimental results are compared with theoretical calculations performed by the use of EMPIRE and TALYS codes. Sensitivity of the calculations to characteristics of nuclear excited states was analyzed.

## 1. Introduction

Determination of the cross sections of *(n, xγ)* reactions induced by interaction of fast neutrons with nuclei of the reactor constructive materials is of special importance for the calculations of the γ-ray fields in the active zone of the reactors. These cases are important for estimation of energy release and γ-ray radiation shielding. The cross sections values are also needed for investigation of different nuclear reaction mechanisms in the neutron induced reactions as well as characteristics of nuclear excited states and their decay.

Despite of numerous experimental measurements performed by neutrons with 14 MeV energy, data on γ-spectra in full energy range (up to excitation energy of the nucleus) in the same experiment are absent. In this contribution we present results of the γ-spectra measurements from *(n, xγ)* reactions on $^{nat}Cd$ within the energy interval from 2 to 18 MeV. Measurement results are compared with theoretical calculations allowing gamma-emission from compound nucleus states and preequilibrium states.

## 2. Experimental measurements and data analysis

The measurements of γ-spectra are performed using the scintillation γ-spectrometer based on 15x10 cm NaI(Tl) detector. The geometry of the experiment is presented on Fig. 1.

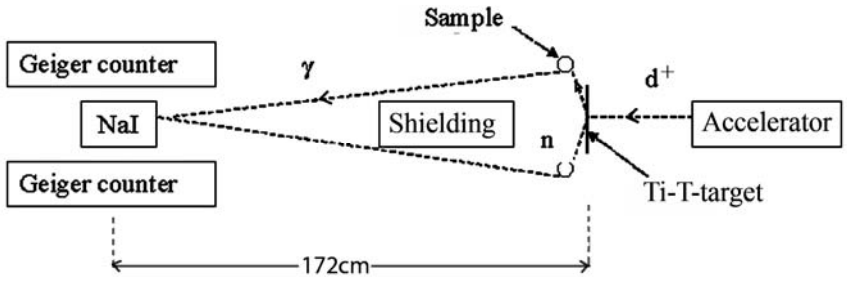


Fig. 1. Geometry of the experiment.

Time-of-flight method based on pulse neutron generator was applied for separation of prompt γ-rays from source neutrons, background and rescattered γ-rays. Reaction T($d$, $n$)$^4$He in Ti-T target was used as neutron source. Deuterons were accelerating by low-voltage accelerator with klystron bunching of deuteron beam and finally deuteron energy was 130 keV. Pulse generation frequency was equal to 7.25 MHz, average neutron intensity ~ $10^7$ $s^{-1}$. Measurements were performed with neutrons of energy 14.0±0.2 MeV which corresponds to the angle 90 ° on deuteron beam. Neutron source was placed in the centre of ring sample of cadmium with radius 16 cm. The Geiger counters were used in anti-coincidence with spectrometer signals in order to reduce the influence of cosmic rays. The flight path between the neutron source and NaI(Tl) detector was equal to 172 cm which provides reliable separation of prompt γ-rays from neutron and γ-ray background (Fig.2). More details concerning experiment can be found in Refs. [1-3].

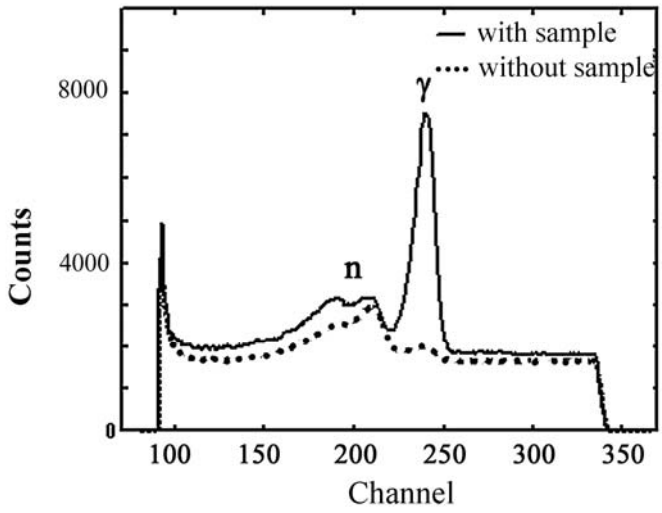


Fig. 2. Time separation of the prompt γ-rays and background neutrons: solid curve — spectrum, obtained with sample, dashed curve – without sample.

Relation between amplitude spectra $A(V,\Delta V,\theta_\gamma)$ and differential cross section $\sigma_\gamma(E_\gamma,\theta_\gamma) \equiv d^2\sigma(E_\gamma,\theta_\gamma)/dE_\gamma d\Omega_\gamma$ is given by the expression

$$A(V,\Delta V,\theta_\gamma) = \int_0^{E_{max}} R(V,E_\gamma)\cdot\sigma_\gamma(E_\gamma,\theta_\gamma)dE_\gamma, \qquad (1)$$

where $V$ is signal amplitude; $\Delta V$ is signal amplitude width; $\theta_\gamma$ is scattering angle; $E_\gamma$ is γ-ray energy; $E_{max}=E_n+S_n$, where $E_n$ is energy of incident neutron, $S_n$ is neutron separation energy of composite nucleus;

$$R(V,E_\gamma) = \int_{V-\Delta V/2}^{V+\Delta V/2} G\alpha_\gamma(E_\gamma)\varepsilon(V,E_\gamma)dV\,. \qquad (2)$$

Here, $G$ is geometry factor; $\alpha(E_\gamma)$ is energy-depended coefficient of the γ-ray self-absorption by sample detector; $\varepsilon(V, E_\gamma)$ is detector response function. The expression for the detector

response function $\varepsilon(V, E_\gamma)$ was taken from Ref. [4]. It is based on analytical approximation of the bremsstrahlung experiment with correction on Monte Carlo simulations as well as on detection of 4.43 MeV γ-rays from neutron inelastic scattering on carbon.

Amplitude spectrum have been measured at $\theta_\gamma = 90°$; which gives cross sections $\sigma_\gamma(E_\gamma, \theta_\gamma = 90°)$ . Because of weak angular dependence of the differential cross sections the quantity $4\pi\sigma_\gamma(E_\gamma, \theta_\gamma = 90°)$ can be considered as angle-integrated energy spectrum

$$\frac{d\sigma(E_\gamma)}{dE_\gamma} \equiv \sigma(E_\gamma) = 4\pi \cdot \sigma_\gamma(E_\gamma, \theta_\gamma = 90°). \qquad (3)$$

We use this expression for determination of experimental data on angle-integrated γ-spectrum.

Eq. (1) is Fredholm integral equation of the first kind. There are problems in its solving due to instability of unfolded spectra to the experimental data uncertainties (so called ill-posed). Algorithm on the compact set of limited variations with set of monotonically decreasing functions [5] was used to find cross sections. Uncertainties of the cross sections were estimated in assumption that the amplitude spectrum is distributed with Gauss distributions due to the large number of external factors; then additional unfolding procedures were used [3]. Sensitivity of the unfolded cross sections to variation of detector response functions was also analyzed. It was obtained that variation of response function within interval of 10-15% leads to changes of cross sections values not more then 5-7%.

Experimental values of the unfolded differential cross sections and their uncertainties are shown on Fig. 3.

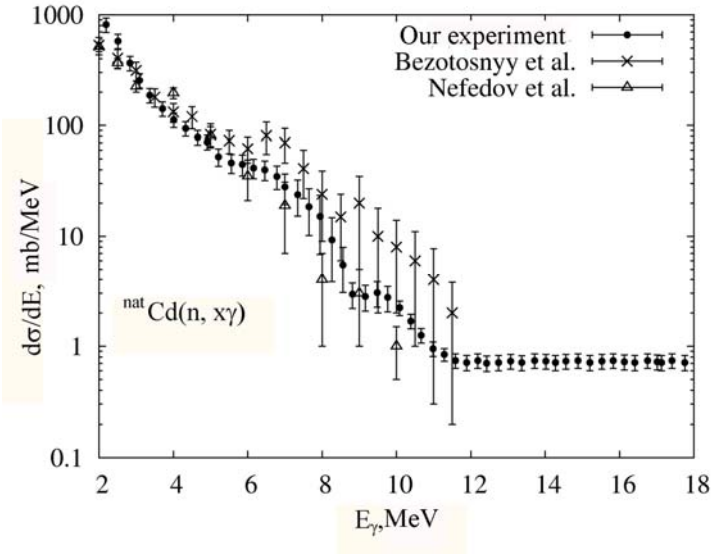


Fig. 3. Differential cross sections of the reactions $^{nat}Cd(n, x\gamma)$ obtained using regularization algorithm on the compact set of limited variations: points – results of our experiment, crosses – experimental data from [6], triangles – [7].

Rather good agreement of measured cross sections with results from Ref. [6, 7] is obtained.

### 3. Results of the theoretical calculations

Experimental results were compared with theoretical calculations of inclusive γ-spectrum which corresponds to the sum of spectra for all possible reactions with incident neutron:

$$\frac{d\sigma(n,x\gamma)}{dE_\gamma} = \frac{d\sigma(n,\gamma)}{dE_\gamma} + \sum_j \frac{d\sigma(n,jb,\gamma)}{dE_\gamma} + \sum_k \frac{d\sigma(n,\gamma,kc)}{dE_\gamma} + \dots , \qquad (4)$$

where $j$ and $k$ are the numbers of emitted particles $b$, $c$ of different kind ($b, c = n, p, d, t, \alpha$) determined by conservation laws.

Theoretical calculations performed using EMPIRE (version 3.0) [8] and TALYS (version 1.2) [9] codes with allowing emissions from compound nucleus and preequilibrium nuclear states. The Hauser-Feshbach model was used in the calculations of emission from compound nuclei and the exciton model was applied from calculations of preequilibrium emission. the following input parameters are required for cross section calculations[10]: nuclear level density, optical potential and radiative strength function (RSF).

Fig. 4 shows experimental differential cross sections of the reactions $^{nat}$Cd(n, xγ) in comparison with theoretical calculations. In case of EMPIRE code, the following input parameters were used in the calculations [12]: dipole electric RSF (E1 RSF) within model of modified Loretzian (MLO) and Enhanced Generalized Super-Fluid Model (EGSM) for the nuclear level densities. In TALYS code E1 RSF was calculated within Enhanced Generalized Loretzian (EGLO) with Gilbert-Cameron approach for nuclear level densities. These set of parameters are used in corresponding codes as default ones. The following isotopes of cadmium were considered in the calculations: $^{106}Cd$ (12 %), $^{108}Cd$ (0,9 %), $^{110}Cd$ (12,4 %), $^{111}Cd$ (12,8 %), $^{112}Cd$ (24 %), $^{113}Cd$ (12,3 %), $^{114}Cd$ (28,8 %) and $^{116}Cd$ (7,6 %) where abundances of corresponding isotopes are indicated in brackets. Calculated values of cross sections for each isotope were summed in accordance with their abundances to obtain cross sections of reactions on $^{nat}Cd$ .

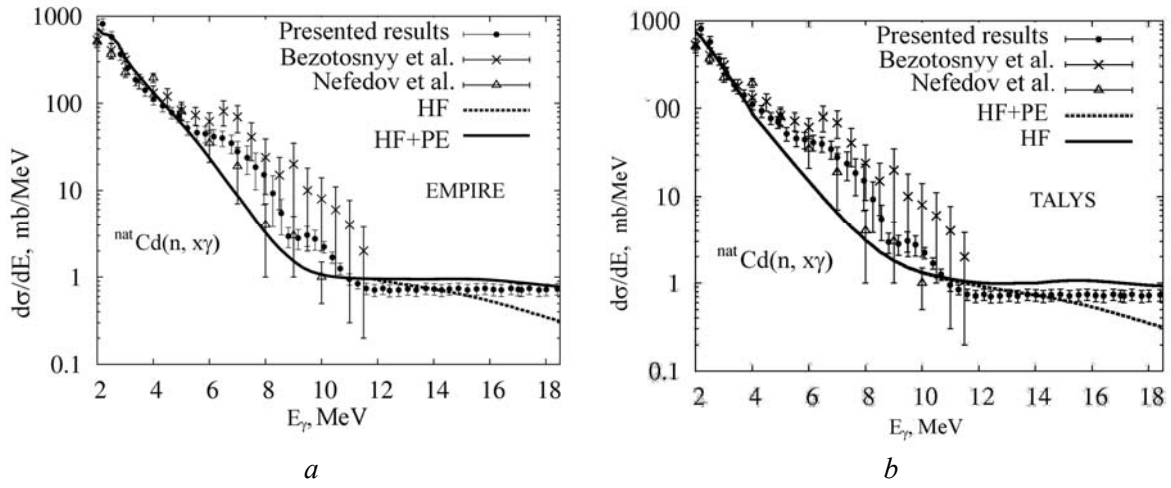


Fig. 4. Differential cross sections of the reactions $^{nat}Cd(n, x\gamma)$ performed using EMPIRE *(a)* and TALYS *(b)* codes: points – our experimental results, solid curve – calculations within Hauser - Feshbach model, dashed curve – calculations within Hauser - Feshbach model with taking into account preequilibrium emission (PE).

As one can see from Fig.4, rather satisfactory agreement of the theoretical calculations with experimental data is obtained for the $^{nat}Cd(n, x\gamma)$ reactions almost in all energy range accept interval from 6 MeV to 11 MeV, where experimental results exceed theoretical ones. It is also can be concluded that taking into account preequilibrium processes gives the better agreement of experimental data and theoretical calculations for the energy range above 12 MeV. Calculations within EMPIRE and TALYS codes are in rather good agreement.

Sensitivity of the calculated cross sections to input parameters mentioned above was analyzed. Calculations were performed with using EMPIRE code. Fig. 5 demonstrates the cross sections obtained by the use of different optical potentials taken from [11-13]. It can be seen from Fig. 5 that theoretical results obtained using all potentials gives rather same agreement of theoretical calculations with experimental results.

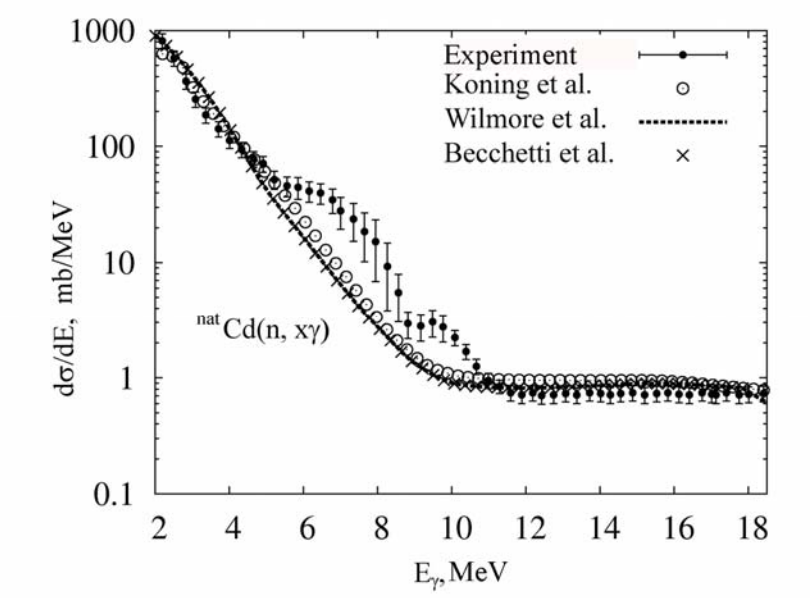


Fig. 5. Differential cross section of the reactions $^{nat}Cd(n, x\gamma)$ calculated with EMPIRE code using different optical potentials: points – our experimental results, circles – Koning potential [11], dashed curve – Wilmore potential [12], crosses – Becchetti potential [13].

To check sensitivity of the cross sections to the different approaches for nuclear level densities the following models were used: Enhanced Generalized Super-Fluid Model (EGSM), Back-Shifted-Fermi-Gas Model (BSFG) and Gilbert-Cameron approach (GC). More detailed description of all the models mentioned above can be found in Ref. [10]. Fig. 6 demonstrates the example of the dependence of $^{nat}Cd(n, x\gamma)$ reaction cross sections on nuclear level density.

It can be seen from Fig. 6 that theoretical results obtained using both EGSM and BSFG models gives rather same agreement of theoretical calculations with experimental results.

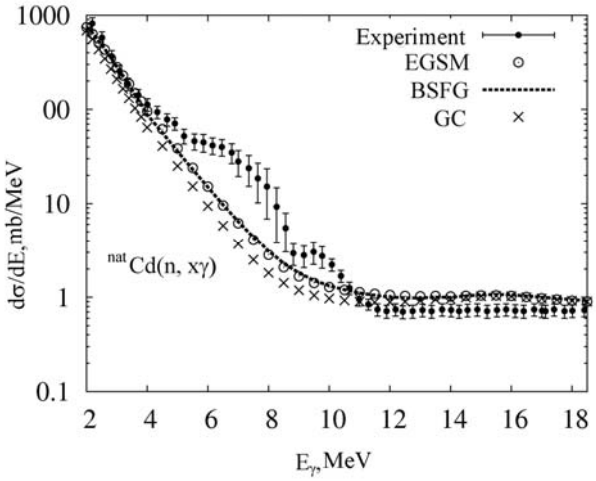


Fig. 6. Differential cross sections of the $^{nat}Cd(n, x\gamma)$ reactions calculated with EMPIRE code using different models different models for the nuclear level densities: open circles – EGSM model, dashed curve – BSFG model, crosses – Gilbert-Cameron approach. Experimental results are shown by points.

We also checked sensitivity of the calculations to the shape of electric dipole RSF. Calculations were performed using the following models: Standart Loretzian (SLO), Enhanced Generalized Loretzian (EGLO), modified Loretzian (MLO), Generalized Fermi liquid (GFL) model [11, 14-16]. EGSM model was used for the nuclear level densities. Results of the calculations are shown on Fig. 7.

As one can see, the best agreement with the experiment is obtained in case of using SLO and MLO models for radiative strength function.

It was also checked that calculated cross sections are insensitive to the high values of the γ-ray transition multipolarity. It is caused by the fact that number of the nuclear levels is large and electric dipole transitions are dominated.

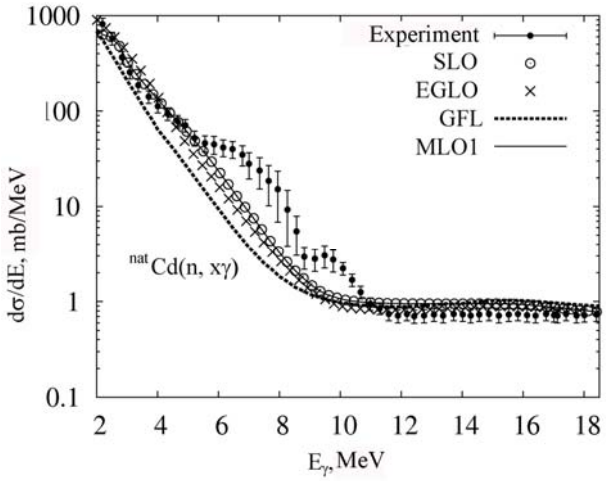


Fig. 7. Differential cross sections of the $^{nat}Cd(n, x\gamma)$ reactions calculated with EMPIRE code using different models for the RSF : open circles – SLO model, crosses – EGLO, dashed curve – GFL, solid line – MLO. Experimental results are shown by points.

From the results presented on Figs. 5-7, one can conclude that good agreement of the theoretical calculations with experimental results can be obtained in the case of simultaneous changes of the models both the nuclear level density and E1 radiative strength function.

## 4. Conclusions

Differential cross sections of $^{nat}Cd(n, x\gamma)$ reactions were measured using time-of-flight technique. The algorithm on the compact set of limited variations was used in order to obtain the cross sections values and their uncertainty estimations.

The experimental results are compared with theoretical calculations performed with allowing emission of γ-rays and particles from equilibrium and preequilibrium nuclear states. It was demonstrated that taking into account preequilibrium processes gives the best agreement of experimental data and theoretical calculations. Results of the calculations are rather in good agreement with experimental data except energy region from 6 to 11 MeV. Disagreement within this interval can be caused by some effect of nuclear structure on the input parameters, especially on nuclear level density.

In order to obtain the best agreement of calculated cross sections with experimental results, the optimal set of models for nuclear level densities, potential and RSF should be used. According to our analysis, cross sections of $^{nat}Cd(n, x\gamma)$ reactions calculated by the use SLO and MLO models for radiative strength functions and with EGSM for the nuclear level densities lead to the best agreement with experimental results.

**Acknowledgments.** O.M. Gorbachenko expresses his deep gratitude to the Organizing Committee of the Conference for financial support and warm welcome.

REFERENCES

1. V. M. Bondar, I. M. Kadenko, B. Yu. Leshchenko et al., *Reactor Dosimetry State Of The Art 2008: Proc. 13th Int. Symp.* (25-30 May, 2008, Alkmaar, Netherlands), (2009) 516.
2. V. M. Bondar, I. M. Kadenko, B. Yu. Leshchenko et al., Bull. Russian Acad. Sciences: Physics, **73(11**) (2009) 1511.
3. B. M. Bondar, V. M. Bondar, O.M. Gorbachenko et al., Nuclear Physics and Atomic Energy, **12(2)** (2011) 129.
4. G. M. Gurevich, V. M. Mazur, G. V. Solodukhov, Instr. Exp. Techn., **2** (1975) 59.
5. A. N. Tikhonov, A. V. Goncharsky, V. V. Stepanov et al., Numerical methods for the solution of ill-posed problems, Moscow, 1990 (in Russian).
6. V. M .Bezotosnyi, V. M.Gorbachev, M. A. Efimova et al, Atomic Energy, **4** (1980) 239.
7. Yu.Ya. Nefedov, V.I.Nagornyy, V.I.Semenov et al., Vop. At.Nauki i Tekhn.,Ser.Yadernye Konstanty, **1** (2000) 7.
8. M. Herman, R.Capote, B.V. Carlson et al., Nucl. Data Sheets, **108** (2007) 2655.

9. A. J. Koning, S . Hilaire, M. C. Duijvestijn, In *Proc. of the International Conference on Nuclear Data for Science and Technology*, ND2007 (April 22 – 27, 2007, Nice, France), **1** (2007) 211.
10. R. Capote, M. Herman, M. Oblozinsky et al, Nucl. Data Sheets, **110** (2009) 3107.
11. A.J. Koning, J.P. Delaroche, Nucl. Phys. A713 (2003) 231.
12. D. Wilmore, P. E. Hodgson, Nucl. Phys., **55** (1964) 673 .
13. F. D. Becchetti, G. W. Greenlees, Phys. Rev., **182** (2000) 1190.
14. V. A. Plujko, I. M. Kadenko, O. M. Gorbachenko et al., Int. J. Mod. Phys. E., **17** (2008) 240.
15. V.A. Plujko, R. Capote, O.M. Gorbachenko, At. Nucl. Data Tables, **97** (2011) 567.
16. V.A. Plujko, O.M. Gorbachenko, V.M. Bondar et al., Journal of Korean Physical Society, **59(2)** (2011) 1514.